

Crystal structure of synthetic $\text{Mg}_3\text{Cr}_2\text{Si}_3\text{O}_{12}$, the high-pressure Cr end-member of the knorringite-pyropo garnet series

Amélie Juhin ¹, Guillaume Morin ¹, Erik Elkaim ², Dan J. Frost ³, Farid Juillot ¹, Georges Calas ¹

¹ Institut de Minéralogie et de Physique des Milieux Condensés, UMR CNRS 7590 / Université Paris 6 / Université Paris 7 / IPGP - 140 rue de Lourmel 75015 Paris, France

² Synchrotron SOLEIL, L'Orme des Merisiers, Saint-Aubin - BP 48 91192 Gif-sur-Yvette Cedex, France

³ Bayerisches Geoinstitut, Universität Bayreuth D-95440 Bayreuth, Germany

ABSTRACT

Knorringite, the Cr-end-member of the pyropo garnet series (Nixon et al. 1968), often occur in high proportions in kimberlite garnets and is thus used for tracing high-pressure deep-earth conditions favorable to the formation of diamonds, in which knorringite-rich garnet can occur as inclusions. However, although the synthesis of knorringite is reported in the literature (Ringwood 1977; Irifune et al. 1982; Taran et al. 2004), the structure of the pure end-member has not been yet determined from experimental data. In this study, the crystal structure of knorringite, $\text{Mg}_3\text{Cr}_2(\text{SiO}_4)_3$, has been refined from high resolution synchrotron X-ray powder diffraction data recorded under ambient conditions on a polycrystalline sample synthesized at 12 GPa in a multi-anvil apparatus. The structure is cubic, space group $Ia-3d$, $a = 11.5935(1)$, $V = 1558.27(4) \text{ \AA}^3$, $d_{\text{calc}} = 3.97 \text{ g.cm}^{-3}$. The Cr-O distance of $1.957(2) \text{ \AA}$ is consistent with EXAFS results on the same sample. This short distance indicates a substantial compression of the CrO_6 octahedron, compared to ambient pressure Cr^{3+} -minerals such as uvarovite ($\langle \text{Cr-O} \rangle = 1.99 \text{ \AA}$, Andrut and Wildner 2002). Our experimental results thus confirm early empirical predictions based on series of high-pressure Cr-garnet end-members (Fursenko 1981), showing that the values of the Cr-O distance and the Cr-O-Si angle decrease with the augmentation of pressure and with the diminution of the size of the divalent cation.

INTRODUCTION

Knorringite $\text{Mg}_3\text{Cr}_2\text{Si}_3\text{O}_{12}$, the Cr-end-member of the pyrope garnet series, is an important component of garnets in deeper parts of the upper mantle (Irifune et al. 1982). It often occurs in high proportions in kimberlite garnets: thus, the Cr-concentration is used for tracing high-pressure deep-earth conditions favorable to the formation of diamonds, in which knorringite-rich garnet can occur as inclusions. The highest knorringite content known so far for natural garnets inclusions in diamonds from kimberlites is 66.4 mole % (Stachel and Harris 1997). However, the structure of the knorringite end-member has not been still refined. It has been predicted from the structure of natural garnets using empirical laws involving the radii of the cations (Novak and Gibbs. 1971) and by performing least-square refinement of the interatomic distances (Ottonello et al. 1996). Even more recently, first-principles calculations based on Density Functional Theory have been performed (Milman et al. 2001), but the theoretical structure is in disagreement with the predictions. In particular, the calculated Cr-O distance (1.976 Å) is larger than the two predicted ones (1.958 Å and 1.960 Å).

The remaining uncertainty on the structure of knorringite certainly prevents to complete the investigation of the thermodynamical and structural properties associated with the incorporation of chromium in garnets. For example, the Cr-O distance in Cr-containing pyrope was found to be 1.96 Å (Juhin et al, 2008), but the extension of the structural relaxation (identified as a partial or full process) depends on the Cr-O distance taken for the knorringite end-member.

The synthesis of knorringite is reported by several studies (Ringwood 1977; Irifune et al. 1982; Taran et al. 2004). The space group (*Ia-3d*) and the lattice parameter (11.600(1) Å, Ringwood 1977; 11.596(1) Å, Irifune et al. 1982) have been determined from X-ray diffraction data, but the crystal structure has not been still refined. In this study, we report new results on the crystal structure of knorringite, $\text{Mg}_3\text{Cr}_2\text{Si}_3\text{O}_{12}$ obtained from high resolution synchrotron X-ray powder diffraction data on a synthetic sample. The sample was synthesized in a multi-anvil apparatus at $P = 12$ GPa and $T = 1500^\circ\text{C}$. The Rietveld refined distances are compared to those obtained from Extended X-ray Absorption Fine Structure (EXAFS) measurements performed at the Cr K-edge on the same sample. Finally, the crystal structure of $\text{Mg}_3\text{Cr}_2\text{Si}_3\text{O}_{12}$ is compared to that of other Cr-garnet end-members, $\text{Ca}_3\text{Cr}_2\text{Si}_3\text{O}_{12}$, $\text{Fe}_3\text{Cr}_2\text{Si}_3\text{O}_{12}$ and $\text{Mn}_3\text{Cr}_2\text{Si}_3\text{O}_{12}$.

MATERIALS AND EXPERIMENTAL

High-pressure synthesis

Starting materials were stoichiometric mixtures of dried MgO, Cr₂O₃ and noncrystalline SiO₂. The starting mixtures plus 1 μ L of water were encapsulated in Re capsules, which were enclosed in the high-pressure cell of an octahedral multianvil apparatus. The two synthesis runs were performed at the Bayerisches Geoinstitut (University of Bayreuth, Germany), using a 1000-ton press and a 14M sample assembly of tungsten carbide anvils. The samples were heated using a LaCrO₃ furnace and the temperature was controlled to $\pm 1^\circ\text{C}$ using a W₉₇Re₃ / W₇₅Re₂₅ thermocouple. Run conditions, which are reported in Table 1, are close to those of Taran et al. (2004). The experimental calibrated pressures are given ± 0.3 GPa. The samples were quenched by switching off the power to the furnace, with of quench rate $> 200^\circ\text{C}\cdot\text{s}^{-1}$. The run products were examined under a binocular microscope. In order to get a rough estimate of their composition, powder x-ray diffraction patterns were recorded using a Panalytical X'Pert Pro MPD diffractometer with CuK α radiation. In both samples referred to as *Kn-1* and *Kn-2*, knorringite was found to be the major phase, associated to a small (similar) amount of eskolaite (α -Cr₂O₃) and to traces of stishovite (SiO₂).

X-ray powder diffraction using synchrotron radiation

A high-resolution x-ray powder diffraction-pattern of the synthetic *Kn-1* sample was recorded in 3 h in transmission Debye-Scherrer geometry at the CRISTAL undulator beamline at the SOLEIL synchrotron facility, Saclay, France. Approximately 10 mg of sample were mounted in a rotating silica capillary 300 μm in diameter. The pattern was recorded within the $6 - 60^\circ 2\theta$ range with a wavelength of 0.7285 \AA . The diffracted beam was collected using a Ge(111) analyser leading to an instrumental peak width lower than $0.02^\circ 2\theta$ which was evaluated by recording a few Bragg peaks of the LaB₆ powder diffraction standard.

EXAFS experiments

Approximately 10 mg of sample *Kn-2* were finely grinded together with cellulose, in order to make a pellet. Two Cr K-edge X-ray Absorption spectra were collected at room temperature on beamline BM30b (FAME), at the European Synchrotron Radiation Facility (Grenoble, France) operated at 6 GeV. Calibration was made with respect to the first inflection point in a Cr metal foil (5989 eV). The data were recorded using the fluorescence mode with a Si (220) double crystal and a Canberra 30-element Ge detector (Proux et al. 2006), with a spacing of 0.5 eV and of 0.05 \AA^{-1} respectively in the XANES and EXAFS regions.

EXAFS data were corrected for self-absorption and extracted using the XAFS program (Winterer 1997). Radial distribution functions around the Cr absorber were obtained by calculating the Fourier transform (FT) of the $k^3\chi(k)$ EXAFS function using a Kaiser–Bessel window within the 2–15 Å⁻¹ k -range with a Bessel weight of 2.5. Least-squares fitting of the unfiltered $k^3\chi(k)$ functions was performed with the planewave formalism, using a Levenberg–Marquard minimization algorithm. Theoretical phase-shift and amplitude functions employed in this fitting procedure were calculated with the curved-wave formalism using the FEFF 8 code (Ankudinov et al. 1998) and the knorringite predicted structure (Novak and Gibbs 1971). The fit quality was estimated using a reduced χ^2 of the following form:

$$\chi_{FT}^2 = \frac{N_{ind}}{n(N_{ind} - p)} \sum_{i=1}^n (\|FT\|_{exp_i} - \|FT\|_{calc_i})^2, \text{ where } N_{ind} \text{ is the number of independent parameters}$$

($N_{ind} = \frac{2\Delta k \Delta R}{\pi}$), p the number of free fit parameters, n the number of data points fitted, and $\|FT\|_{exp}$ and $\|FT\|_{calc}$ the experimental and theoretical Fourier transform magnitude within the [0.5–6 Å] R -range of the k^3 -weighted EXAFS signal. The number of allowable independent parameters is 45, and our fit included at most 15 variable parameters.

RESULTS AND DISCUSSION

Structure refinement

The structure was Rietveld refined from the experimental synchrotron X-ray powder-diffraction pattern in the range 6–60° 2θ , using the program XND (Berar and Baldinozzi 1998). Absorption for Debye Scherrer geometry (Rouse et al. 1970) was negligible for $\mu_r = 0.3 \text{ cm}^{-1}$ (assuming that the apparent density of the powder would be half that of the mineral). Scale factors, cell parameters and width and shape parameters of pseudo-Voigt line-profile functions were refined for knorringite $\text{Mg}_3\text{Cr}_2\text{Si}_3\text{O}_{12}$, eskolaite $\alpha\text{-Cr}_2\text{O}_3$ and stishovite SiO_2 . Atom parameters of these two latter phases were kept fixed to the literature values (Newnham and deHaan 1962; Ross et al. 1990). Indeed, quantitative analysis derived from scale factor values, using the classical method without internal standard (Bish and Post 1989) indicated that eskolaite and stishovite weight fraction in the sample were $10 \pm 2 \text{ wt}\%$ and $\sim 1 \text{ wt}\%$, respectively. For knorringite, all atom positions and displacement parameters were refined, together with site occupancies of the cations, using the predicted structure (Novak and Gibbs 1971) as starting model. About 174 Bragg reflections from knorringite were fit in the 6–60° 2θ range and the R_{wp} parameter for the pattern and the R_{Bragg} parameter for knorringite reached final values of 0.125 and 0.037, respectively (Table 2). Final atom positions, displacement parameters, and site occupancies are reported in Table 3.

The Rietveld refined interatomic distances are similar to those determined from predictions based on least-square refinement procedure in a series of natural samples (Novak and Gibbs 1971; Ottonello et al. 1996): in particular, the Rietveld refined Cr-O distance is equal to 1.957(2) Å, close to the respective values of 1.958 Å and 1.960 Å predicted by these authors. However, it is significantly shorter than the Cr-O distance derived from first-principles calculation (1.976 Å, Milman et al. 2001). The Cr-Mg / Cr-Si distance (3.240 (2) Å) determined from the present Rietveld analysis is close to both the distances predicted by Novak and Gibbs (1971) and Ottonello et al. (1996), i.e. 3.253 Å and 3.243 Å, respectively, and the theoretical one derived from first-principles calculation (3.255 Å).

EXAFS experiments

Chromium K-edge k^3 -weighted EXAFS signal for the synthetic sample is shown in Fig. 2a, and the corresponding Fourier transform is displayed in Fig. 2b. Table 5 lists the results of the fit performed on the $k^3\chi(k)$ EXAFS data. The first neighbor contribution was fitted with 4.8 oxygen atoms at 1.96 ± 0.02 Å, which corresponds to the Cr-O distance in knorringite, in good agreement with the refined one. No attempt was made to fit it with an additional contribution of the Cr-O scattering paths in eskolaïte, because of the low proportion of this minority phase in the synthetic samples. Moreover, the Cr-O mean distance in eskolaïte (1.99 Å) is too close to that in knorringite to be resolved by EXAFS analysis.

The second peak observed in the Fourier transform (Fig. 2b) between 2.1-3.5 Å is due to a mixed contribution of Cr-Si/Cr-Mg single scattering paths in knorringite and Cr-Cr paths in eskolaïte. The fitted Cr-Si/Cr-Mg distance is $3.25 \text{ Å} \pm 0.04 \text{ Å}$, which is in good agreement with the value obtained by Rietveld refinement. The Cr-Cr distances in eskolaïte were fit to $2.94 \text{ Å} \pm 0.04 \text{ Å}$ and $3.69 \text{ Å} \pm 0.04 \text{ Å}$, which are larger than those derived from the structure refinement by Newnham and deHaan (1962), i.e., 2.89 Å and 3.65 Å, respectively. This discrepancy, and the fact that the number of neighbors obtained by our EXAFS analysis is underestimated in both structures, can be likely explained by the significant overlap of the different contributions. The third peak observed on the Fourier transform between 4.1-5.3 Å is due to Cr-Cr and Cr-Si/Cr-Mg pair correlations in knorringite, at $5.01 \pm 0.04 \text{ Å}$ and $5.23 \pm 0.04 \text{ Å}$, respectively. The fit distances are again similar to the refined ones (5.020(2) Å and 5.225(2) Å). Thus, we can conclude that the results of our EXAFS experiments are consistent with the interatomic distances obtained from Rietveld refinement of knorringite.

Comparison between the crystal structure of high-pressure Cr-garnet end-members

The most common Cr-garnet end-member is uvarovite $\text{Ca}_3\text{Cr}_2\text{Si}_3\text{O}_{12}$, which can be synthesised at ambient pressure (Andrut and Wildner 2002). Apart from $\text{Mg}_3\text{Cr}_2\text{Si}_3\text{O}_{12}$, which can be obtained above approximately $P=11$ GPa (Irifune et al. 1982), two other Cr-garnet end-members, $\text{Mn}_3\text{Cr}_2\text{Si}_3\text{O}_{12}$ and $\text{Fe}_3\text{Cr}_2\text{Si}_3\text{O}_{12}$, were obtained from synthesis runs performed at high pressure (respectively, above $P=2$ GPa

and 6 GPa, Fursenko 1981). The necessity to increase the synthesis pressure seems to be related to the decrease of the ionic radius of the dodecahedral divalent cation ($r(\text{Ca}^{2+}) = 1.12 \text{ \AA}$, $r(\text{Mn}^{2+}) = 0.96 \text{ \AA}$, $r(\text{Fe}^{2+}) = 0.92 \text{ \AA}$ and $r(\text{Mg}^{2+}) = 0.89 \text{ \AA}$) (Fursenko 1981). Although the crystal structures of $\text{Mn}_3\text{Cr}_2\text{Si}_3\text{O}_{12}$ and $\text{Fe}_3\text{Cr}_2\text{Si}_3\text{O}_{12}$ have not been yet refined, they have been predicted (Novak and Gibbs 1971; Ottonello et al. 1996). The respective lattice parameters are in good agreement with the values measured from X-ray powder diffraction data (Fursenko 1981). As in the case of knorringite, the predicted structures are similar to the one we obtained in the present work by Rietveld refinement, we can infer that the predictions made on the structures of $\text{Mn}_3\text{Cr}_2\text{Si}_3\text{O}_{12}$ and $\text{Fe}_3\text{Cr}_2\text{Si}_3\text{O}_{12}$ also yield valuable information. Therefore, we used the predicted structures given by Ottonello et al. (1996) for these two garnets and the refined structures of $\text{Ca}_3\text{Cr}_2\text{Si}_3\text{O}_{12}$ (Andrut and Wildner 2002) and $\text{Mg}_3\text{Cr}_2\text{Si}_3\text{O}_{12}$ to better understand the effect of pressure on structural changes in these garnet series. The evolution of the Cr-O distance and the Cr-O-Si angle, together with the minimum pressure of synthesis, is plotted in Figures 3a and 3b, respectively. The Cr-O distance decreases when the synthesis pressure increases, showing a significant compression of the CrO_6 octahedron. Additionally, the Cr-O-Si angle decreases by 3.7 % from uvarovite to knorringite, while in the mean time, the Si-O distance decreases by 1.5 % ($\langle\text{Si-O}\rangle = 1.6447 \text{ \AA}$ in $\text{Ca}_3\text{Cr}_2\text{Si}_3\text{O}_{12}$ vs $\langle\text{Si-O}\rangle = 1.620 \text{ \AA}$ in $\text{Mg}_3\text{Cr}_2\text{Si}_3\text{O}_{12}$). This confirms that the compression of the garnet structure is achieved by the rotation of the SiO_4 tetrahedra, rather than by their deformation (Ungaretti et al. 1995).

ACKNOWLEDGMENTS

The authors are very grateful to G. Gudfinnsson for help in the preparation of the high-pressure synthesis runs. These experiments were performed at the Bayerisches Geoinstitut under the EU "Research Infrastructures: Transnational Access" Programme (Contract No. 505320 (RITA) - High Pressure).

REFERENCES

- Andrut, M. and Wildner M. (2002) The crystal chemistry of birefringent natural uvarovites. Part III. Application of the superposition model of crystal fields with a characterization of synthetic cubic uvarovite. *Physics and Chemistry of Minerals*, 29, 595-608.
- Ankudinov A. L., Ravel B., Rehr J. J. and Conradson S. D. (1998) Real-space multiple-scattering calculation and interpretation of X-ray-absorption near-edge structure. *Physical Review B* 58, 7565–7576.
- Berar J.F. and Baldinozzi G. (1998) XND code: From X-ray laboratory data to incommensurately modulated phases. Rietveld modelling of complex materials. *International Union of Crystallography- Commission for Powder Diffraction Newsletter* 20, 3-5.

- Bish D.L. and Post J.E. (1989) Modern Powder Diffraction, *Reviews in Mineralogy*, vol. 20, D.L. Bish and J.E. Post, editors, Mineralogical Society of America.
- Brown, I.D. and Altermatt, D. (1985) Bond-Valence parameters obtained from a systematic analysis of the inorganic crystal structure database. *Acta Crystallographica* B41, 244-247.
- Fursenko, B. A. (1981) Synthesis of new high pressure garnets: $Mn_3Cr_2Si_3O_{12}$ and $Fe_3Cr_2Si_3O_{12}$. *Bulletin de Minéralogie*, 104, 418-422
- Irifune, T., Ohtani, E., and Kumozawa, M. (1982) Stability field of knorringite $Mg_3Cr_2Si_3O_{12}$ at high pressure and its implication to the occurrence of Cr-rich pyrope in the upper mantle. *Physics of the Earth and Planetary Interiors*, 27, 263-272.
- Juhin, A., Calas, G., Cabaret, D., Galois, L., and Hazemann, J.L. (2008) Structural relaxation around substitutional Cr^{3+} in pyrope garnet. *American Mineralogist*, 93, 800-805. Milman, V., Akhmatkaya, E. E., Nobes, R. H., Winkler, B., Pickard, C. J., and White, J. A. (2001) Systematic *ab initio* study of the compressibility of silicate garnets, *Acta Crystallographica* B57, 163-177.
- Newnham, R.E. and deHaan, Y.M. (1962) Refinement of the $\alpha-Al_2O_3, Ti_2O_3, V_2O_5$ and Cr_2O_3 structures. *Zeitschrift für Kristallographie*. 117, 235-237.
- Nixon P.H., Hornung G. (1968) A new chromium garnet end member, knorringite, from kimberlite. *American Mineralogist*, 53, 1833-1840.
- Novak, G. A. and Gibbs, G. V. (1971) The crystal chemistry of the silicate garnets. *American Mineralogist*, 56, 791-825.
- Ottonello, G., Bokreta, M. and Sciuto, P.F. (1996) Parametrization of energy and interaction in garnets : end-member properties. *American Mineralogist*, 81, 429-447.
- Proux O., Nassif V., Prat A., Ulrich O., Lahera E., Biquard X., Menthonnex J.J., and Hazemann J.L. (2006) Feedback system of a liquid nitrogen cooled double-crystal monochromator: design and performances. *Journal of Synchrotron Radiation*, 13, 59-68.
- Ringwood, A. E. (1977) Synthesis of pyrope-knorringite solid solution series. *Earth and Planetary Science Letters*, 36, 443-448.
- Ross N.L., Shu J-F., Hazen R.M., Gasparik T. (1990) High-pressure crystal chemistry of stishovite. *American Mineralogist* 75, 739-747.
- Rouse, K.D., Cooper, M.J., York, E.J. and Chakera, A. (1970) Absorption correction for neutron diffraction. *Acta Crystallographica* A26, 682-691.
- Stachel T., Harris J.W. (1997) Syngenetic inclusions in diamond from the Birim field (Ghana) - a deep peridotitic profile with a history of depletion and re-enrichment. *Contributions to Mineralogy and Petrology*, 127, 336-352.

- Taran, M.N., Langer, K., Abs-Wurmbach, I., Frost, D.J., and Platonov, A.N. (2004) Local relaxation around $^{6}\text{Cr}^{3+}$ in synthetic pyrope-knorringite garnets, $^{8}\text{Mg}_3^{6}(\text{Al}_{1-x}\text{Cr}_x^{3+})_2^{4}\text{Si}_3\text{O}_{12}$, from electronic absorption spectra. *Physics and Chemistry of Minerals*, 31, 650-657.
- Ungaretti, L., Leona, M., Merli, M., and Oberti, R. (1995) Non-ideal solid solutions in garnet: crystal-structure evidence and modeling. *European Journal of Mineralogy*, 7, 1299-1312.
- Winterer M. (1997) XAFS—a data analysis program for materials science. *Journal de Physique IV*, 7, 243–244.

FIGURES AND TABLES

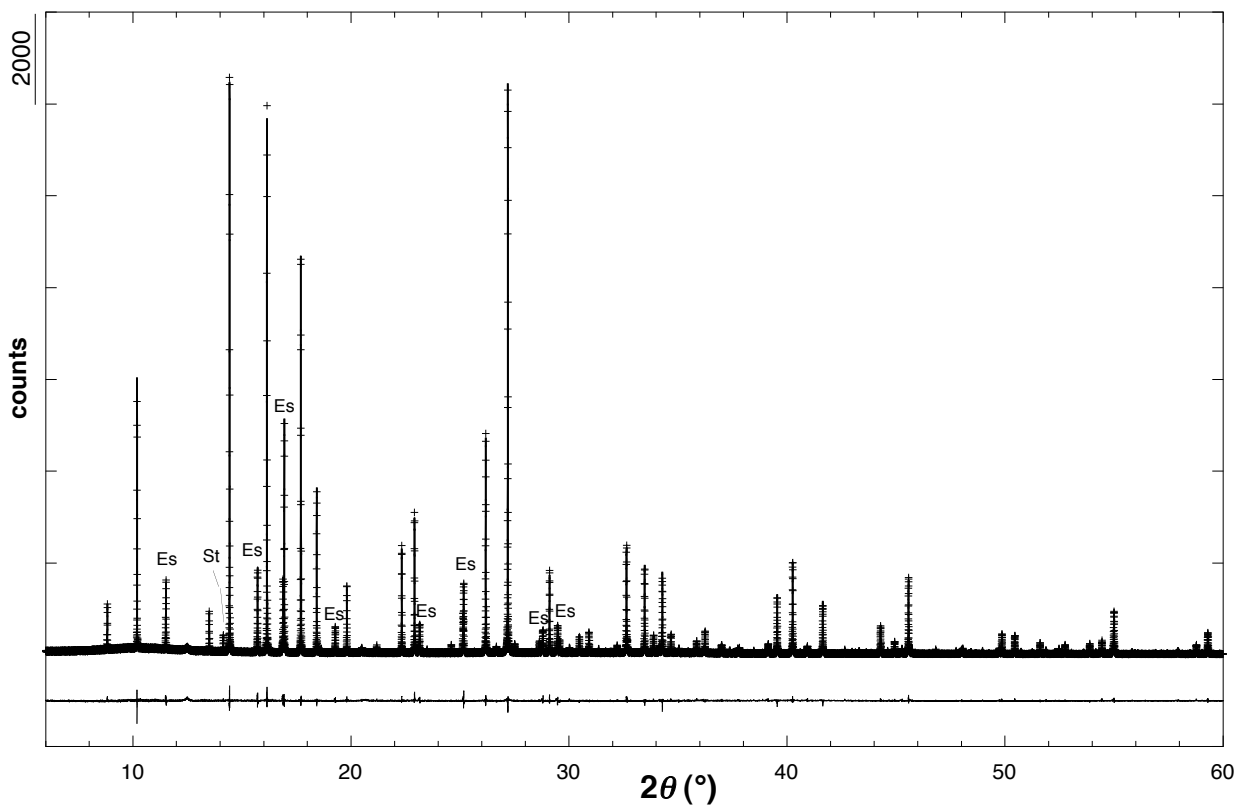


Figure 1. Rietveld refinement of the X-ray powder pattern of the knorringite sample. Experimental data (crosses), calculated (solid line), difference (thin solid lines). The main Bragg reflections of the eskolaite (Es) and stishovite (St) mineral impurities are indicated.

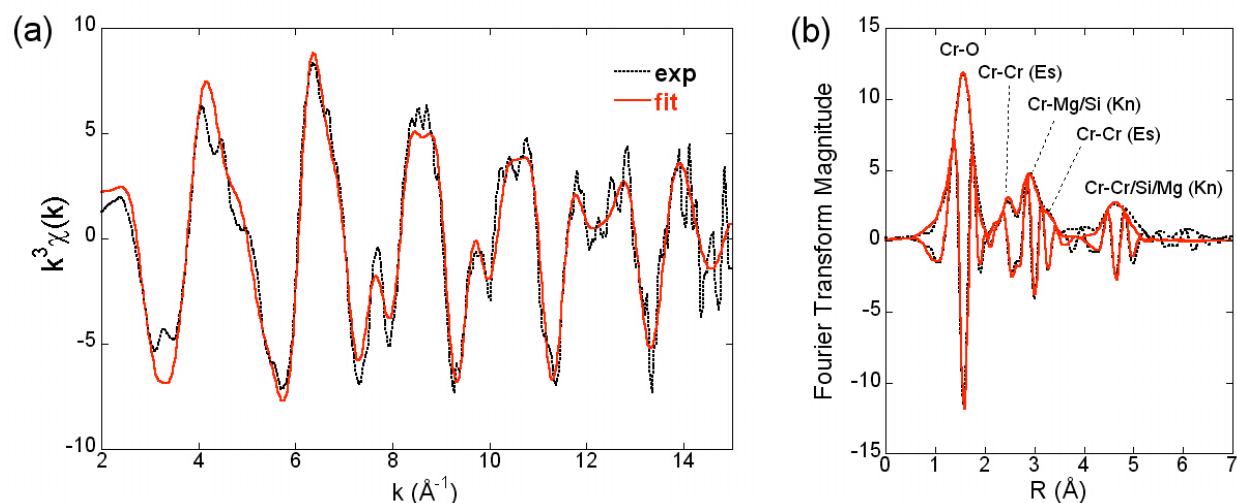


Figure 2. Cr K-edge unfiltered EXAFS data recorded at 293 K for synthetic knorringite sample: (a) k^3 -weighted EXAFS, and (b) its corresponding Fourier transforms (FT), including the magnitude and imaginary part of the FT. Experimental and calculated curves are displayed as dashed and solid lines, respectively. All fit parameters are provided in Table 5.

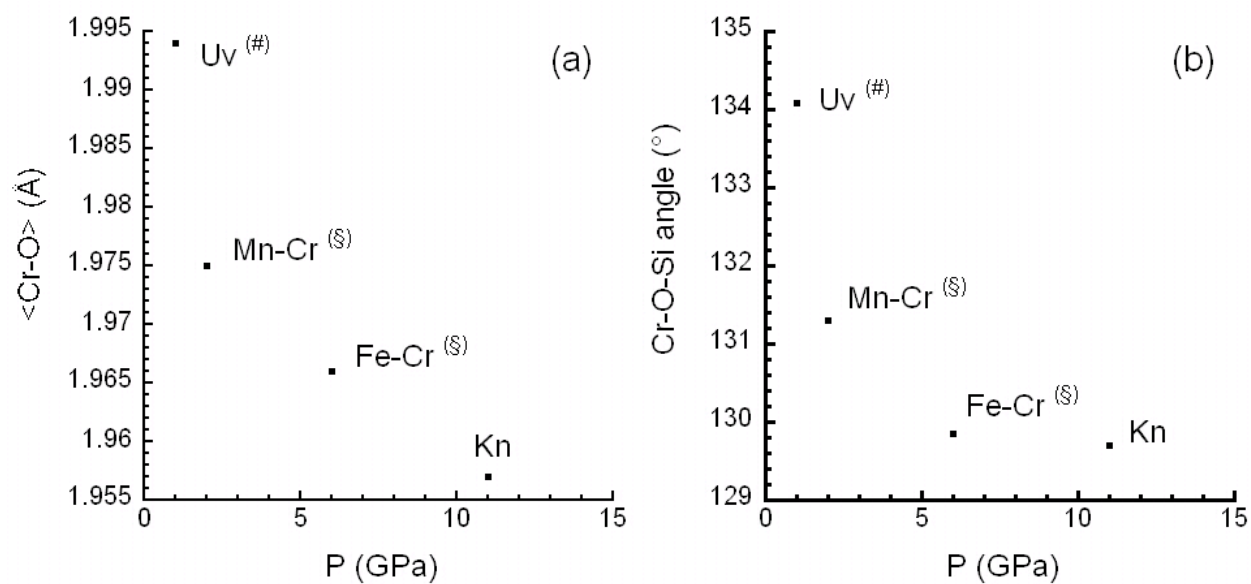


Figure 3. (a) Dependence of $\langle \text{Cr-O} \rangle$ distance (\AA) vs minimum pressure of synthesis (GPa) for Cr-garnet end members. (b) Dependence of Cr-O-Si angle ($^\circ$) vs pressure of synthesis (GPa). Uv: $\text{Ca}_3\text{Cr}_2\text{Si}_3\text{O}_{12}$, Mn-Cr: $\text{Mn}_3\text{Cr}_2\text{Si}_3\text{O}_{12}$, Fe-Cr: $\text{Mn}_3\text{Cr}_2\text{Si}_3\text{O}_{12}$ and Kn: $\text{Mg}_3\text{Cr}_2\text{Si}_3\text{O}_{12}$. #: Andrut and Wildner (2002), §: calculated from Ottonello et al (1996).

Table 1. Conditions and results of high-pressure multianvil runs. The following abbreviations are used : Kn : knorringite, Es : eskolaïte, St : stishovite. The run numbers are those of the diary of the Bayerisches Geoinstitut.

Run n°	label	P (GPa)	T (°C)	Duration (h)	Appearance	Phases
H2732	<i>Kn-1</i>	11	1500	5	Dark green	Kn + Es (+St)
H2733	<i>Kn-2</i>	14	1600	6	Dark green	Kn + Es (+St)

Table 2. Structure-refinement parameters for knorringite

Formula	$\text{Mg}_3\text{Cr}_2(\text{SiO}_4)_3$
Formula weight (g/mol)	453.21
No. of structural formula in cell unit	8
Space group	<i>Ia-3d</i>
<i>a</i> (Å)	11.5935(1)
Unit-cell volume, <i>V</i> (Å ³)	1558.37(4)
Temperature	Ambient
Wavelength (Å)	0.7285
Step increment (2θ)	0.0015
Geometry	Debye-Scherrer
Background	Spline
Profile function	pseudo-Voigt
Pattern range (2θ)	6 - 60
Number of reflections	174
Refined parameters	21
Rwp (%) overall	12.4
Rp (%) overall	8.6
Goodness of fit overall	1.11
R_{Bragg} (%)	3.7

Table 3. Atomic parameters for knorringite: fractional coordinates, isotropic Debye-Waller factor (B_{iso}), occupancy factor (Occ) and site multiplicity (Mult). Standard deviations on the last digit are under brackets.

Atom	x/a	y/b	z/c	B_{iso} (\AA^2)	Occ	Mult
Mg ²⁺	1/8	0	1/4	1.00(8)	1.03(1)	24
Cr ³⁺	0	0	0	0.31(3)	0.93(1)	16
Si ⁴⁺	3/4	0	1/4	0.64(6)	1.03(1)	24
O ²⁻	0.0345(2)	0.0517(2)	0.6569(2)	0.76(6)	1	96

Table 4. Selected distances (\AA) and angles ($^\circ$) in CrO₆/MgO₈/SiO₄ polyhedra for knorringite. Standard deviations on the last digit are under brackets.

	Distance (\AA)	Angle ($^\circ$)
Cr-O	1.957(7) x 6	
O-O (unshared)	2.811(7) x 6	91.8(1)
O-O (Mg-shared)	2.722(7) x 6	88.2(1)
Si-O	1.620(8) x 4	
O-O (Mg-shared)	2.469(7) x 2	99.3(1)
O-O (unshared)	2.730(7) x 4	114.8(1)
Mg-O _a	2.223(6) x 4	
Mg-O _b	2.363(6) x 4	
O _a -O _a (Si shared)	2.469(7) x 2	67.4(1)
O _a -O _b (Cr shared)	2.722(7) x 4	72.8(1)
O _b -O _b (unshared)	2.786(8) x 2	72.2(1)
O _a -O _b (Mg shared)	2.695(7) x 4	71.9(1)

Table 5. Results of multi-shell fit of EXAFS data for the knorringite synthetic sample. ($\chi^2_{FT}=0.38$). R (Å): interatomic distance, N : number of neighbors, σ (Å): Debye-Waller factor, ΔE_0 (eV): difference between the user-defined threshold energy and the experimentally determined threshold energy. During the fitting procedure, all parameter values indicated by (--) were linked to the parameter value placed above in the table. Error on R value is estimated as ± 0.02 Å for the Cr-O distance and ± 0.04 Å for the other distances. Errors on N , σ and ΔE_0 values are estimated respectively as ± 0.5 , ± 0.01 and ± 0.3 , respectively.

phase		R (Å)	N	σ (Å)	ΔE_0 (eV)
Knorringite (Kn)	Cr-O	1.96	4.8	0.062	4.71
Knorringite (Kn)	Cr-Si	3.25	2.7	0.032	--
Knorringite (Kn)	Cr-Cr	5.01	1.7	--	--
Knorringite (Kn)	Cr-Si	5.23	2.8	--	--
Eskolaïte (Es)	Cr-Cr	2.94	0.7	0.065	--
Eskolaïte (Es)	Cr-Cr	3.69	0.8	--	-